

1           **Estimating Surface Carbon Fluxes Based on a Local Ensemble**  
2           **Transform Kalman Filter with a Short Assimilation Window and a**  
3           **Long Observation Window: an OSSE test in GEOS-Chem 10.1**

4  
5       <sup>1,2</sup> Yun Liu, <sup>1</sup>Eugenia Kalnay\*, <sup>1</sup>Ning Zeng\*, <sup>3</sup> Ghassem Asrar, <sup>4</sup>Zhaohui Chen, <sup>5</sup>Binghao  
6       Jia

7  
8       1 Dept. of Atmospheric and Oceanic Science, University of Maryland – College Park

9       2 Dept. of Oceanography, Texas A & M university, College Station, TX

10       3 Joint Global Change Research Institute/PNNL, College Park, MD

11       4 School of Environmental Science, University of East Anglia, Norwich, UK

12       5 State Key Laboratory of Numerical Modeling for Atmospheric Sciences and  
13       Geophysical Fluid Dynamics (LASG), Institute of Atmospheric Physics, Chinese

14       Academy of Sciences, Beijing, China

15

16

17       \*Corresponding authors: [ekalnay@umd.edu](mailto:ekalnay@umd.edu), [zeng@umd.edu](mailto:zeng@umd.edu)

18

19

20

21

22

23

24

25

26

27

28

29

30

31

32

33

34

35

36

37

38

39

40

41

42

43

44

1  
2  
3  
4  
5  
6  
7  
8  
9  
10  
11  
12  
13  
14  
15  
16  
17  
18  
19  
20  
21  
22  
23  
24  
25  
26  
27  
28  
29  
30  
31  
32

**Abstract**

We developed a Carbon data assimilation system to estimate the surface carbon fluxes using the Local Ensemble Transform Kalman Filter and atmospheric transport model GEOS-Chem driven by the MERRA-1 reanalysis of the meteorological field based on the Goddard Earth Observing System Model, Version 5 (GEOS-5). This assimilation system is inspired by the method of Kang et al. [2011, 2012], who estimated the surface carbon fluxes in an Observing System Simulation Experiment (OSSE) as evolving parameters in the assimilation of the atmospheric CO<sub>2</sub>, using a short assimilation window of 6 hours. They included the assimilation of the standard meteorological variables, so that the ensemble provided a measure of the uncertainty in the CO<sub>2</sub> transport. After introducing new techniques such as “variable localization”, and increased observation weights near the surface, they obtained accurate surface carbon fluxes at grid point resolution. We developed a new version of the LETKF related to the “Running-in-Place” (RIP) method used to accelerate the spin-up of EnKF data assimilation [Kalnay and Yang, 2010; Wang et al., 2013, Yang et al., 2014]. Like RIP, the new assimilation system uses the “no-cost smoothing” algorithm for the LETKF [Kalnay et al., 2007b], which allows shifting at no cost the Kalman Filter solution forward or backward within an assimilation window. In the new scheme a long “observation window” (e.g., 7-days or longer) is used to create an LETKF ensemble at 7-days. Then, the RIP smoother is used to obtain an accurate final analysis at 1-day. This new approach has the advantage of being based on a short assimilation window, which makes it more accurate, and of having been exposed to the future 7-days observations, which improves the analysis and accelerates the spin up. The assimilation and observation windows are then shifted forward by one day, and the process is repeated. This reduces significantly the analysis error, suggesting that the newly developed assimilation method can be used with other Earth system models, especially in order to make greater use of observations in conjunction with models.

Key words: Carbon Data Assimilation, Surface Carbon Flux, LETKF

1  
2  
3  
4  
5  
6  
7  
8  
9  
10  
11  
12  
13  
14  
15  
16  
17  
18  
19  
20  
21  
22  
23  
24  
25  
26  
27  
28  
29  
30  
31

## 1. Introduction

The exchange of carbon among the atmosphere, land and oceans contributes to changes in the Earth’s climate, and is also sensitive to climate conditions. The CO<sub>2</sub> concentration in the atmosphere is affected by both the natural variability of the Earth’s planetary system, and anthropogenic emissions. The terrestrial and oceanic ecosystems absorb more than one-half of the anthropogenic CO<sub>2</sub> emission [Le Quéré *et al.*, 2016]. One major scientific question is whether this rate of removal of CO<sub>2</sub> from atmosphere will continue in future, and can it be enhanced? It is thus essential to better quantify the dynamics of earth surface carbon fluxes (SCF), and the variations of carbon sources and sinks, and their associated uncertainties.

A common approach for estimating SCF from atmospheric CO<sub>2</sub> measurements and atmospheric transport models is referred to as a “top-down” approach. The “top-down” methods estimate SCF through techniques such as Bayesian synthesis approach [Rödenbeck *et al.*, 2003; Gurney *et al.*, 2004; Enting, 2002; Bousquet *et al.*, 1999], different types of ensemble Kalman filters (EnKF) [e.g. Peters *et al.*, 2005, 2007; Feng *et al.*, 2009; Zupanski *et al.* 2007; Lokupitiya *et al.*, 2008], or variational data assimilation method [e.g., Baker *et al.*, 2006, 2010; Chevallier *et al.*, 2009].

Kang *et al.* [2011, 2012] developed a “top-down” carbon data assimilation system by coupling an atmospheric general circulation model (AGCM), including atmospheric CO<sub>2</sub> concentrations, with the Local Ensemble Transform Kalman Filter (LETKF) [Hunt *et al.*, 2007]. The meteorological variables (wind, temperature, humidity, surface pressure) and CO<sub>2</sub> concentrations were assimilated simultaneously in order to account for the uncertainties of the meteorological field, and their impact on the transport of atmospheric CO<sub>2</sub>. They carried out Observing System Simulation Experiments (OSSEs), and their carbon assimilation system achieved for the first time an accurate estimation of the evolving SCF at the model grid resolution, without requiring any *a priori* information. The surface carbon fluxes were considered as “unobserved evolving parameters”, by augmenting the state vector at each column with a surface carbon flux (SCF). The Local Ensemble Transform Kalman Filter (LETKF) then estimated this evolving parameter from the error covariance between the low level atmospheric CO<sub>2</sub> and the estimated SCF,

1 and after a spin-up of about one month, the LETKF accurately recovered the nature run  
2 seasonal surface carbon fluxes.

3 Kang et al., [2011, 2012] used a short 6-hour assimilation window for both  
4 atmospheric and CO<sub>2</sub> observations because atmospheric observations are usually  
5 assimilated at this frequency, and because most Ensemble Kalman Filter methods require  
6 short windows to ensure that the forecast perturbation growth remains linear. Such a short  
7 data assimilation window, required by the LETKF, also protects the system from  
8 becoming ill conditioned [Enting, 2002, Fig. 1.3], and as a result it does not require  
9 additional *a priori* information. We note further that the use of such a short assimilation  
10 window differs very much from most other “top-down” approaches for estimating SCF  
11 that use long assimilation windows varying from a few weeks to months or even years  
12 [e.g., Baker et al., 2006, 2010; Peters et al., 2005, 2007; Michalak, 2008; Feng et al.,  
13 2009, Liu et al, 2016].

14 Although the Kang et al. methodology was successful, it is computationally  
15 expensive, requiring ensemble forecasts and data assimilation not only for the carbon  
16 variables, but also for the standard atmospheric variables, in order to estimate the  
17 uncertainties of the CO<sub>2</sub> atmospheric transport process. In this study, we used an  
18 improved version of LETKF data assimilation system with a state-of-the-art atmospheric  
19 transport model, the GEOS-Chem [Bey et al., 2001; Nassar et al., 2013], which is driven  
20 by the MERRA-1 reanalysis of the Goddard Earth Observing System Model, Version 5  
21 (GEOS5). The improved data assimilation system, unlike Kang et al [2011, 2012], does  
22 not include an estimation of transport uncertainties related to the meteorological field.

23 The ultimate goal of our LETKF\_C system is to estimate the grid-point SCFs,  
24 which, as in Kang et al. [2011, 2012], are treated as time-evolving parameters in the  
25 system. As mentioned before, an Ensemble Kalman Filter requires a short assimilation  
26 window in order to have the ensemble perturbations evolve linearly and remain Gaussian.  
27 On the other hand, it is well known that the training needed to estimate evolving  
28 parameters through data assimilation could be quite long, so that it benefits from having  
29 many observations. Therefore, a short assimilation window would shorten the training  
30 period needed for the estimation of the SCF error covariance, and therefore lengthen the  
31 spin-up time.

1 To address this problem, we developed a new version of the LETKF using the  
2 “Running-in-Place” (RIP) method to accelerate the spin-up of EnKF data assimilation  
3 [Kalnay and Yang, 2010; Wang et al., 2013; Yang et al., 2012]. Like RIP, the new  
4 assimilation system uses the “no-cost smoothing” algorithm [Kalnay et al., 2007b] that  
5 allows shifting at a negligible cost the Kalman Filter solution forward or backward within  
6 a given assimilation window. Briefly, the new scheme works like this: a long  
7 “observation window” (e.g., 7-days, containing all the observations within 7 days) is used  
8 to create a temporary LETKF ensemble analysis at 7-days. Then the RIP smoother is  
9 used to obtain a final analysis at 1-day. This analysis has the advantage of being based on  
10 a short assimilation window, which makes it more accurate, and of having been exposed  
11 to the 7-days of observations, which accelerates the spin up time. The assimilation and  
12 observation windows are then shifted forward by one day, and the process is repeated.  
13 We have tested this new method (short assimilation, long observation window) achieving  
14 a significant reduction of analysis errors, and we believe that this method could be useful  
15 in other data assimilation problems.

16 This paper is organized as follows: Section 2 briefly describes the new system  
17 used for CO<sub>2</sub> data assimilation (LETKF\_C). Section 3 explores the effect of combining  
18 assimilation and observation windows in an OSSE framework. Section 4 presents results  
19 of the proposed methodology applied to CO<sub>2</sub> data. A summary and discussion are  
20 presented in section 5.

## 21 22 **2. LETKF\_C data assimilation system**

23 A data assimilation system includes a forecast model, observations, and a data  
24 assimilation method that optimally combines them. In the proposed LETKF\_C data  
25 assimilation system we use the GEOS-Chem as the forecast model and LETKF as the  
26 data assimilation method. The pseudo-observations for our OSSE experiments are  
27 created at the locations of the real carbon observations from Orbiting Carbon  
28 Observatory-2 (OCO-2) satellite [Crisp et al., 2004].

### 29 30 **2.1 GEOS-Chem model and the “nature” run**

31 GEOS-Chem is a global 3-D atmospheric Chemical transport model driven by the

1 NASA reanalysis (MERRA-1) meteorological fields from the Goddard Earth Observing  
2 System data assimilation Version 5, by the NASA Global Modeling and Assimilation  
3 Office [Bosilovich et al., 2015]. This model has been applied worldwide to a wide range  
4 of atmospheric composition and transport studies. The GEOS-Chem model used in this  
5 study is the version v10-01 with a resolution of  $4^\circ \times 5^\circ$  (latitude x longitude), and 47  
6 hybrid pressure-sigma vertical levels for CO<sub>2</sub> simulation [Nassar et al., 2013]. GEOS-  
7 Chem is driven by the MERRA-1 reanalysis with 72 hybrid vertical levels, extending  
8 from the surface up to 0.01 hPa. The data used in this study was provided by the GEOS-  
9 Chem support team, based at the Harvard and Dalhousie Universities with support from  
10 the NASA Earth Science Division and the Canadian National and Engineering Research  
11 Council, who re-gridded the original data of spatial resolution of  $0.25^\circ \times 0.3125^\circ$  into the  
12 resolution of  $4^\circ \times 5^\circ$ .

13 GEOS-Chem requires the SCFs as a set of parameters at each grid point in order  
14 to simulate the CO<sub>2</sub> concentration in the atmosphere. It is not possible to observe the  
15 global SCFs directly. Therefore, the SCFs are created from a “bottom-up” approach  
16 (considered as “truth” in our experiments) and used for the simulation of atmospheric  
17 CO<sub>2</sub> concentration with GEOS-Chem. The “bottom-up” SCFs used in this study include  
18 the three components shown in Equation (1): 1) terrestrial carbon fluxes ( $F_{TA}$ ); 2) air-sea  
19 carbon fluxes ( $F_{OA}$ ); 3) anthropogenic fossil fuel emissions ( $F_{fe}$ ).

$$20 \quad SCF = F_{TA} + F_{OA} + F_{fe} \quad (1)$$

21 The  $F_{TA}$  values are derived from the VEgetation Global Atmosphere Soils (VEGAS)  
22 model [Zeng et al., 2004; Zeng et al., 2005], forced by the real evolving weather,  
23 obtained from the GEOS-Chem. The  $F_{OA}$  values are from Takahashi et al. [2002], a  
24 climatological seasonal cycle estimated for the 1990s, and the  $F_{fe}$  values are from Fossil  
25 Fuel Data Assimilation System (FFDAS) for the year 2012 [Asefi-Najafabady et al.,  
26 2014]. The air-sea carbon flux and  $F_{fe}$  values were scaled using the global carbon budget  
27 data of Le Quéré et al. [2015], in order to include interannual variations. A nature run for  
28 atmospheric CO<sub>2</sub> concentration simulation is driven by the SCFs in units of  $\left(\frac{kgC}{m^2yr}\right)$  based  
29 on all three datasets.

30 In OSSEs, the nature run serves as the “truth”. We assume that the true “bottom-

1 up” carbon fluxes are not known in our data assimilation experiments, and they will be  
2 estimated using the atmospheric pseudo-observations derived from the “truth”, as  
3 described in more detail below. The nature run obtained by coupling GEOS-Chem with  
4 VEGAS is fairly realistic [figure not shown], so we use it to create the pseudo OCO-2  
5 observations for the period of January 2015- March 2016.

## 6 **2.2 Pseudo-Observations**

7 The ultimate goal of this model-data assimilation system is to estimate the SCFs  
8 at every grid point using real observations such as the conventional surface CO<sub>2</sub>  
9 measurements of GlobalViewplus (GV+) flask network provided by Cooperative Global  
10 Atmospheric Data Integration Project [2016], and the observations from satellites such as  
11 the Greenhouse Gases Observing Satellite (GOSAT) [Yokota et al., 2004], and the  
12 Orbiting Carbon Observatory-2 (OCO-2) [Crisp et al., 2004]. Therefore, it is very  
13 beneficial to choose a realistic observation network to generate the pseudo-observations  
14 for testing the proposed data assimilation system. In this study, we developed the pseudo-  
15 observations for the OSSE assimilation experiments based on a realistic OCO-2  
16 observation product.

17 The OCO-2 observations are the CO<sub>2</sub> column-averaged dry air mole fractions  
18 over the entire OCO-2 pixel (defined as XCO<sub>2</sub>). The synthetic observations cover the  
19 entire globe once every 14 days with very high spatial resolution. It includes 24 samples  
20 per second along the satellite track within ~ 7 km span. The observations are expected to  
21 be highly correlated over a short length scale. Furthermore, the observation quality is  
22 greatly affected by conditions such as cloud cover, surface type and the solar zenith angle  
23 at the time of measurement. The OCO-2 retrieval algorithm uses a warning level (WL)  
24 between 0 and 19 to indicate the quality of measurements, where WL=0 means “most  
25 likely good”, and WL=19 means “least likely good” observations. To avoid highly  
26 correlated measurements being treated as independent measurements and to bring the  
27 spatial resolution in line with the resolution of atmosphere transfer model, David Baker  
28 provided an OCO-2 observation dataset which averaged the synthetic XCO<sub>2</sub> in 10-  
29 second time window using the “good quality” observations retrieval defined by WL<=15  
30 (D. Baker, personal communication).

31 The OCO-2 retrievals used to obtain averages are based on the NASA Atmospheric

1 CO2 Observations from Space XCO2 retrieval Algorithm version7r (O'Dell et al., 2012),  
2 as archived at [https://disc.gsfc.nasa.gov/datasets/OCO2\\_L2\\_Lite\\_FP\\_7r/summary](https://disc.gsfc.nasa.gov/datasets/OCO2_L2_Lite_FP_7r/summary) (last  
3 access: 23 March 2017). A two-step averaging method has been used in order to avoid  
4 the final average to be disproportionately weighted to one part of the averaging bin (track)  
5 with more good quality retrievals. In the first step, the “good quality” retrievals defined  
6 as  $WL \leq 15$  and  $XCO2\_quality\_flag = 0$  (another quality indicator of the data) are  
7 averaged over 1-second bins, with weights inversely proportional to the square of each  
8 retrievals posterior uncertainty. In the second step, all the 1-second bins, with at least one  
9 valid retrieval, are averaged over a 10-second interval to create 10-second averaged data.  
10 The OCO-2 averaging kernels are similarly averaged to create 10-second mean averaging  
11 kernels. This averaging method had been used for similar purposes in the recent study by  
12 Basu et al. (2018). In this study, we further aggregated the observations from David  
13 Baker at the nearest GEOS-Chem output time of the 0, 6, 12, 18 UTC for each model day.  
14 The typical one-day coverage of observation of OCO-2 is shown in Figure 1. The values  
15 of XCO2 in the winter are significantly larger than those in summer of the Northern  
16 hemisphere and the OCO-2 observations are missing in the winter, for middle and high  
17 latitude regions (latitude  $> \sim 30$ ). We used the actual location, time and error scales of the  
18 OCO-2 observations to create the pseudo-observations for our experiment. The pseudo-  
19 observations are created by obtaining the “true” CO2 from the “nature” run using the  
20 location and time of the valid observation, then adding random errors with due  
21 consideration to the scales of the corresponding real observations. These derived pseudo-  
22 observations used in this study are based on the real observations associated error scales,  
23 thus are much more realistic than the GOSAT observations also used in Kang et al.  
24 [2012], because they are anchored, on the real OCO-2 observations and on their quality,  
25 and their statistical representation.

26

### 27 **2.3 The LETKF data assimilation system**

28 The ensemble Kalman filter (EnKF) is a powerful tool for data assimilation that  
29 was first introduced by Evensen [1994]. The key attribute of this method is to derive the  
30 forecast uncertainties from an ensemble of integrated model simulations. A variety of  
31 ensemble Kalman filter assimilation methods have been proposed [Burgers et al., 1998;



1 Houtekamer and Mitchell, 1998; Anderson, 2001, 2003; Bishop et al., 2001; Whitaker  
 2 and Hamill, 2002; Tippett et al., 2003; Ott et al., 2004, Hunt et al., 2004]. The Local  
 3 Ensemble Transform Kalman Filter (LETKF) introduced by Hunt et al. [2007] is chosen  
 4 for this study.

5 The LETKF is an extension of the Local Ensemble Kalman Filter [Ott et al., 2004]  
 6 with the implementation of the ensemble transform filter [Bishop et al., 2001; Wang and  
 7 Bishop, 2003]. It is widely used for data assimilation, including several operational  
 8 centers, and was also used for carbon data assimilations by Kang et al. [2011, 2012].

9 As discussed earlier, we follow Kang et al., [2011] in estimating the SCFs as  
 10 evolving parameters, augmenting the state vector  $C$  (the prognostic variable of  
 11 atmospheric CO<sub>2</sub>) with the parameter SCF, i.e.,  $X = [C, SCF]^T$ . The analysis mean  $\bar{X}^a$   
 12 and its ensemble perturbations  $X^a$  are determined by Equations (2.1, 2.2) at every grid  
 13 point, and the ensemble analysis is used as initial conditions for the ensemble forecast in  
 14 the next cycle.

$$15 \quad \bar{X}^a = \bar{X}^b + X^b \tilde{K} (y^o - \bar{y}^b) \quad (2.1)$$

$$16 \quad X^a = X^b [(K - 1) \tilde{P}^a]^{1/2} \quad (2.2)$$

17 Here  $\bar{X}^b$  is the mean of the forecast (background) ensemble members;  $X^b$  is a  
 18 matrix whose columns are the background perturbations of  $X_k^b - \bar{X}^b$  for each ensemble  
 19 member  $X_k^b$  ( $k=1, \dots, K$ ), where  $K$  is the ensemble size;  $y^o$  is a vector of all the  
 20 observations;  $\bar{y}^b$  is the background ensemble mean in observation space ( $\bar{y}^b = H(\bar{X}^b)$ ),  
 21 where  $H$  is the observation forward operator that transforms values in the model space to  
 22 those in the observation space;  $\tilde{P}^a = \left[ (Y^b)^T R^{-1} Y^b + \frac{(K-1)I}{r} \right]^{-1}$  is the analysis error  
 23 covariance matrix *in ensemble space*, which is a function of  $Y^b = H X^b$ , the matrix of  
 24 background ensemble perturbations in the observation space,  $R$ , the observation error  
 25 covariance (e.g., measurement error, aggregation error, representativeness error), and of  
 26  $r$ , a multiplicative inflation parameter; and  $\tilde{K} = \tilde{P}^a Y^b R^{-1}$ . LETKF assimilates  
 27 simultaneously all observations within a certain distance at each analysis grid point,  
 28 which defines the localization scale. Hunt et al. [2004] introduced a 4-dimensional  
 29 version, and Hunt et al. [2007] provide a detailed documentation of the 4D-LETKF  
 30 which we are using.

## 2.4 Choosing the long observation window (OW) and the short assimilation window (AW)

Like other data assimilation methods, LETKF proceeds in analysis cycles that consist of two steps, a forecast step and an analysis step. In the analysis step, the model forecast (also called prior or background) and the observations are optimally combined to produce the analysis (also called the posterior), which is the best estimate of the current state of the system under study. In the forecast step, the model is then advanced in time with the analysis as the initial condition and its result becomes the forecast for the next analysis cycle. All observations within the assimilation time window are used to constrain the state at the end of the assimilation window.

The focus of this study is on the estimation of SCFs that are time varying parameters in GEOS-Chem. As mentioned earlier, a preliminary LETKF analysis, which provides the weights for each ensemble perturbation, is performed over a longer window (e.g., 7 days, with observations starting at time  $t$ ). Then, the “No-Cost” smoothing [Kalnay et al, 2007b, Kalnay and Yang, 2010] is applied, using the same analysis weights obtained at the end of the long observation window (e.g., 7 days) for each ensemble member, but combining the ensemble perturbations at the end of the corresponding short assimilation window (e.g., 1-day). This creates the final 1-day analysis (at time  $t+AW$ ), which benefits from the information from all the observations made throughout the long OW (7 days), and from the linearity of the perturbations in the short AW of 1 day, which is required for accuracy. At this time the procedure is repeated starting at  $t+AW$ , one day later.

In this new approach, we have the flexibility to combine a short assimilation window (AW) of length  $m$  (e.g.,  $m=1$  day), with a long observation window (OW) of length  $n$  (e.g.,  $n=7$  days), to improve the estimation of SCF. In the forecast step, the model is integrated from  $t$  to  $t+n$ , to produce the forecast corresponding to the observations within the OW. In the analysis step, the observations and corresponding forecasts within the OW are used by the LETKF to estimate optimal weights for the ensemble members. The “No-Cost” smoother applies these optimal weights to determine the analysis of the model state and the SCF parameter at  $t + m$ . The resulting analysis is

1 then used as the initial conditions for the next analysis cycle starting from time  $t + m$ .

## 3 **2.5 Experimental setup**

4 In our experiments we used an ensemble size of 20 members, which was  
5 reasonable since the data assimilation include only one state variable (CO2 concentration)  
6 and one parameter variable (SCF). A similar experiment but with 80-member ensemble  
7 size showed only slight improvement of assimilation quality (figure not shown) but  
8 dramatically increased the computational cost. The initial ensemble is created by random  
9 selection of the state and flux values from the model-based “nature” run for both SCF and  
10 atmospheric CO2 concentration. Therefore, the initial uncertainties of fluxes and CO2  
11 values are equivalent to their “natural” variability. Based on a sensitivity analysis, we  
12 found a horizontal localization radius of 15000 km is optimal for our system. Following  
13 Kang et al. [2012], a vertical localization is also applied by assigning a larger weight to  
14 the CO2 updating layers near the surface, to reflect the expected dominance of layers  
15 near the ground in the change of the total column CO2 measured by OCO-2.

## 17 **2.6 Additive Inflation Method**

18 Inflation is very important for our LETKF\_C data assimilation system. The  
19 LETKF uses the forecast ensemble spread to represent forecast uncertainties. All EnKFs  
20 tend to underestimate the uncertainty in their state estimate because of nonlinearities and  
21 limited number of ensemble members (Whitaker and Hamill, 2002). Underestimating the  
22 uncertainty (ensemble spread) leads to overconfidence in the background state estimate,  
23 and less confidence in the observations, which will eventually lead the EnKF to ignore  
24 the observations and result in filter divergence. This is also true for our carbon-LETKF  
25 data assimilation system. The ensemble spread of CO2 in GEOS-Chem model decreases  
26 during model integration when the ensemble members are using the same meteorological  
27 forcing and SCF values, which is very different from the system with prognostic  
28 meteorological fields where the ensemble spread of model state increases during model  
29 integration (not shown). The ensemble spread of SCFs also does not increase during  
30 model integration because the SCFs are predicted using persistence, and the LETKF  
31 decreases the ensemble spreads for both SCFs and CO2 during analysis steps. Therefore,

1 without inflation, the ensemble spread of the CO<sub>2</sub> and SCFs would be continuously  
2 decreasing during data assimilation, and soon would become too small for LETKF to  
3 accept any observations, and hence, cause filter divergence.

4 There are different types of inflation methods that address the problem of  
5 overconfidence, such as multiplicative inflation, relaxation to prior, and additive inflation  
6 [e.g. Anderson and Anderson, 1999; Mitchell and Houtekamer, 2000; Zhang et al., 2004;  
7 Whitaker et al., 2008; Miyoshi, 2011]. For this study, we chose additive inflation, which  
8 adds random fields to the analysis before the ensemble forecast of the next analysis cycle.  
9 Additive inflation has some advantages compared to multiplicative inflation because it  
10 prevents the effective ensemble dimension from collapsing toward the dominant  
11 directions of error growth [Whitaker et al., 2008; Kalnay et al., 2007a]. We applied  
12 additive inflation to the ensemble of atmospheric CO<sub>2</sub> and SCF to increase perturbations  
13 in the initial conditions, for the next time step. It is important for an additive inflation  
14 method to minimize the impact of model imbalance and initial shocks generated by  
15 adding the random fields into a model. Following Kang et al [2012], the added fields are  
16 selected randomly from the model nature run. Pairs of atmospheric CO<sub>2</sub> and surface CO<sub>2</sub>  
17 flux fields are chosen randomly from model nature run within one year before the  
18 analysis time, their ensemble mean is removed and their difference are scaled to a  
19 magnitude corresponding to 30% of model seasonal variance to create the ensemble of  
20 random fields for additive inflation. Therefore, each selected random field is balanced,  
21 and when it is added into model, the balance will be essentially maintained.

### 22 23 **3. Sensitivity analysis for AW and OW length**

24 We tested the new version of the LETKF with short AW and long OW, described  
25 in previous sections by conducting two sets of experiments using the LETKF\_C system  
26 in an OSSE framework with OCO-2 like observations. The first set of experiments used  
27 the regular 4D-LETKF settings (with a single window length AW=OW) to investigate  
28 the effect of the length of AW for estimating SCF. In the second set of experiments, we  
29 investigated the optimal OW length after choosing the best AW from the first set of  
30 experiments. The assimilation period for all experiments was 1 January 2015 to 1 March  
31 2016. The annual mean RMSEs differences are calculated from the simulation results by

1 removing the spin-up period of first two months (January and February 2015). The  
 2 average period is from March 1 2015 to the end of February 2016. The details of  
 3 experimental settings are shown in Table 1.

11 Table 1. Lengths of Assimilation Window (AW), and Observation Window (OW), and  
 12 the resulting time-averaged global mean RMSEs for different experiments. The first four  
 13 experiments use regular 4D-LETKF, with AW=OW. The last four experiments use  
 14 AW=1 day, found to be optimal, and different OWs.

	EXP1	EXP2	EXP3	EXP4	EXP5	EXP6	EXP7	EXP8
AW	6 hours	1 day	3 days	7 days	1 day	1 day	1 day	1 day
OW	6 hours	1 day	3 days	7 days	2 days	8 days	15 days	30 days
RMSE $(\frac{kgC}{m^2yr})$	0.077	<b>0.059</b>	0.068	0.074	0.053	<b>0.041</b>	<b>0.040</b>	0.050

### 16 3.1 Sensitivity analysis for different assimilation windows

17 The sensitivity of SCF estimates to the length of AW was investigated based on  
 18 the first set of experiments (EXP1-EXP4) with regular 4D-LETKF settings, where the  
 19 length of OW is the same as that of the AW. All experiments used the same observations  
 20 and initial conditions. Since the temporal coverage of the OCO-2 observation network is  
 21 too sparse for our LETKF\_C assimilation system to estimate the SCF signal in short time  
 22 scales, we focus on evaluating the estimation of SCF for seasonal and longer time scales.

23 Figure 2 shows the estimated global total surface fluxes from the first set of  
 24 experiments. The “true” global total surface fluxes show a clear seasonal cycle with very  
 25 large carbon uptake during the growing season of Northern Hemisphere (NH), from May

1 to August, and carbon release during other seasons with the peak release during  
2 November. All experiments reproduced fairly well the seasonal cycle of SCF.

3 When the AW is very short (6 hours), there are large magnitude and high  
4 frequency noise overlaying the seasonal cycle. The magnitude of high frequency errors of  
5 SCF estimation in EXP1 is comparable with the seasonal variability of SCF (Figure 2a).  
6 When the AW=7 days, the high frequency errors of estimation decay, but the long  
7 assimilation window increases the analysis RMSE (EXP4). The EXP2 with AW= 1 day  
8 produced the best estimation of SCF among all four experiments with equal observation  
9 and assimilation windows (Figure 2).

10 The advantage of AW=1 day (EXP2) is clearly seen from the smaller average  
11 global root mean square error (RMSE) (Figure 2c). The RMSE of surface carbon flux is  
12 calculated as

$$13 \quad RMSE(t) = \sqrt{E_x((F^a(x, t) - F^n(x, t))^2)} \quad (3)$$

14 where  $x$  and  $t$  are space and time location;  $F^a$  and  $F^n$  indicate the analysis and the “true”  
15 SCF from nature run, respectively.  $E_x$  is spatial average. The estimations from  
16 experiments with long AW (3 days and 7 days) have a smaller RMSE for the first three  
17 months (January to March), when the “truth” had very little variation because the long  
18 AWs enhances the signal and smoothes the high-frequency noise. However, the  
19 experiments with long AW can miss the fine-scale signals of SCF variation and fail to  
20 catch its variations with time. As a result, the estimations with long AW showed large  
21 RMSE during the period when SCF had larger variations. The estimation with AW of 6  
22 hour also showed very large RMSE because of the overwhelming high frequency noise.  
23 Thus the estimation with AW of 1 day had the smallest RMSE among all the experiments  
24 with regular 4D-LETKF.

25 The time-averaged RMSEs of SCFs is calculated as

$$26 \quad RMSE(x) = \sqrt{E_t((F^a(x, t) - F^n(x, t))^2)} \quad (4)$$

27 which shows very similar spatial patterns, but different amplitudes for different  
28 experiments (Figure 3). The large RMSEs of SCF estimation located in Southeast  
29 American, Southeast of China and Russia, resembled that of the SCF variance (not  
30 shown). The regions of higher variance indicate more information is needed to resolve

1 such large variance by observations, which is hard to achieve. As expected, the SCF  
2 RMSE of 0.059 from EXP2 with AW of 1 day is significantly smaller than the RMSE  
3 from EXP1 with a short AW of 6 hour ( $0.077 \frac{kgC}{m^2yr}$ ), and EXP3 and EXP4 with longer  
4 AWs of 3 days ( $0.068 \frac{kgC}{m^2yr}$ ) and 7 days ( $0.074 \frac{kgC}{m^2yr}$ ) respectively.

5 Our results suggest that the optimal AW for estimating SCF is about 1 day. This is  
6 distinctly different from previously published studies that indicate that either a very short  
7 AW (6 hours) [Kang et al 2011, 2012], or a very long AW (longer than a few weeks) are  
8 optimal [e.g., Baker et al., 2006, 2010; Peters et al., 2005, 2007; Michalak, 2008; Feng et  
9 al., 2009]. A short AW can better constrain the model state and therefore produce a  
10 better parameter estimation. However, a very short AW of 6 hours can degrade the SCF  
11 estimation with high frequency noise in our LETKF-C system. We postulate that the high  
12 frequency noise is related to the sampling errors in the CO2-SCF covariance that has  
13 smaller signal-to-noise ratio compared to those in experiments with longer AWs.

14 The same results can be obtained from the same experiments with different initial  
15 times, indicating the robustness of our findings [figure not shown]. The convergence of  
16 estimated SCFs from the experiments starting from months with big SCF variation, such  
17 as April, is slightly slower than the experiments from the time with small SCF variation,  
18 such as January. While the estimated SCFs converges in a few analysis cycles ( a few  
19 days) in our system (Figure 2), the small difference of convergence rate does not make  
20 any significant impact on the quality of estimated SCFs. Moreover, the calculation of  
21 RMSE of estimated SCFs has excluded the spinup period of the first two months to  
22 remove the potential impact of initial conditions and initial time.

23

### 24 **3.2 Sensitivity analysis for different observation windows (OW)**

25 The results presented earlier and associated discussion suggest that parameter  
26 estimation through data assimilation benefits from long training time and having  
27 sufficient number of observations, implying that the length of OW is critical for the  
28 estimation of desired parameter(s). We investigated the effect of such sensitivity to find  
29 out the suitable length of OW for estimating SCF in the second set of experiments  
30 (EXP5-EXP8), all based on the optimum AW=1 day that was identified from the first set

1 of experiments, but now with different OW lengths.

2 The estimated global total SCFs in the second set of experiments show a clear  
3 seasonal cycle matching the “truth” (Figure 4a). Compared with EXP2 (OW=1) shown  
4 with the green line in Figure 2a), EXP5 (OW=2days) reduced the high frequency noise  
5 significantly when the OW length was increased from 1 day to 2 days. There is still some  
6 high frequency noise in the SCF estimation for EXP5, because the observations for 2  
7 days are not sufficient to smooth out the high frequency noise introduced into the  
8 estimation through data assimilation. The estimated global total SCFs for EXP6  
9 (OW=8days), EXP7 (OW=15), EXP8 (OW=30) are much smoother than that of EXP5  
10 (OW=1day), because of their longer OW. However, the estimation for OW of 30 days  
11 shows a clear time shift compared with the “truth”, especially during the transient period  
12 when the majority of ecosystems /plants are switching from dormant phase in the winter  
13 to the growing phase in the spring. The surface carbon fluxes change rapidly during this  
14 period. The time shift can also be seen in the estimations for these experiments with OW  
15 of 15 days, but it is less pronounced. In the proposed LETKF technique, most of  
16 observations in a long OW are introduced at a time later than the assimilation time. Since  
17 the SCFs are temporally evolving parameters, the information (variation) of future  
18 surface fluxes is brought into the estimation of current time when the future observations  
19 are included in the OW. Therefore, the estimated SCF with a very long OW tend to shift  
20 towards its future value. The estimated SCF with moderate OW=8 days and 15 days  
21 (EXP6 and EXP7) are more accurate than those with a short OW of 2 days (EXP5) and  
22 very long OW of 30 days (EXP8), by avoiding the significant high frequent noise  
23 observed in EXP5 (OW=2 days) and the significant time shift present in EXP8, with a  
24 very long observtion window (OW=30 days). The global mean RMSEs of estimated SCF  
25 from OW=8 and 15 days (EXP6 and EXP7) are significantly smaller than those from  
26 OW=2 and 30 days, i.e., EXP5 and EXP8 (Figure 4c).

27 The spatial pattern of time-average RMSE of SCF for EXP5 (OW=2 days; Figure  
28 5) is similar to those in the first set of experiments, which had short AW=OW (Figure 3).  
29 The regions with large RMSE in EXP5 (OW=2 days) disappear with OW=7 and 15 days  
30 in EXP6 and EXP7, because the long OWs enhance the signals for SFC estimation. The  
31 large RMSE in SCF estimates for EXP8 (OW=30 days) are primarily in the Northern



1 Hemisphere mid-latitudes, because of the time shift in estimations with OW=30 days.  
2 The mean RMSEs of experiments with moderate OWs of 8 and 15 days are 0.041  
3  $\frac{kgC}{m^2yr}$  and  $0.040 \frac{kgC}{m^2yr}$ , respectively, which is significantly smaller than those from  
4 experiments with OWs of 2 days ( $0.053 \frac{kgC}{m^2yr}$ ) and 30 days ( $0.050 \frac{kgC}{m^2yr}$ ).

5 However, a longer OW requires a longer forecast period for each forecast step,  
6 which results in additional computational time/cost. For example, EXP7 with OW of 8  
7 days used 8-time more computational time compared to EXP2. Furthermore, the length of  
8 the OW is also constrained by the time scale of estimation parameters. A long OW tends  
9 to generate a time shift for its estimation. For seasonal and longer time scales, OW(s) in  
10 moderate range of 8~15 days appear to be most suitable for the LETKF\_C estimates of  
11 the SCF. EXP6 and EXP7 show almost the same quality of SCF estimation, but EXP6  
12 has higher computational efficiency. The best configuration thus appears to be EXP6  
13 with an OW of 8 days and AW of 1 day, referred as the “benchmark” experiment  
14 hereafter.

15 We note that the high frequency noise in EXP1 with a short AW of 6 hours can be  
16 smoothed out by a long OW (i.e. 8-15 days). We postulate that an experiment with AW  
17 of 6 hours and OW 8 days will produce similarly realistic estimations as the “benchmark”  
18 experiment; however, it would require much more computational time.

19

#### 20 **4 Evaluating estimated fluxes from the “benchmark” experiment**

21 With the moderately long observation and short assimilation windows, we  
22 obtained best estimates of surface carbon fluxes, and their seasonal cycle. This section  
23 describes the SCF estimates from the “benchmark” experiment. Figure 6 shows a  
24 comparison of surface carbon fluxes based on the “benchmark” assimilation experiment  
25 and nature (“truth”) run for Northern Hemisphere Summer (June, July and August) and  
26 Winter seasons (December, January, and February). The “bottom-up” carbon fluxes used  
27 in the “nature” run show a very strong seasonal cycle over the continents, except  
28 Antarctica. The North Hemisphere mid-latitude areas are very large carbon sinks in the  
29 Summer, and carbon sources in the Winter, as expected. The strong seasonal cycle of  
30 surface fluxes mainly related to the variability of terrestrial ecosystems that absorbs large

1 amount of CO<sub>2</sub> during the growing season (Spring and Summer) and release carbon back  
2 to the atmosphere during dormant seasons (Fall and Winter). The estimated surface  
3 fluxes in the seasonal time scale follow closely the “truth”. The benchmark assimilation  
4 experiment closely reproduces the spatial pattern of surface fluxes globally, for different  
5 seasons. The difference between the benchmark estimation and “truth” shown in Figures  
6 6e & 6f are very small. There are some positive carbon flux differences over Northern  
7 Hemisphere mid-latitudes in the Winter, thus a positive bias in estimated atmospheric  
8 CO<sub>2</sub> concentration is expected.

9 The analysis of CO<sub>2</sub> concentrations matches the “nature” run well. The error pattern  
10 also matches the CO<sub>2</sub> seasonal cycle and the error pattern of estimated SCF. Figure 7  
11 shows the comparison of surface atmospheric CO<sub>2</sub> concentrations between the  
12 benchmark assimilation experiment and nature (“truth”) run, for the Northern  
13 Hemisphere Summer and Winter. The spatial pattern of assimilated CO<sub>2</sub> matches the  
14 “truth” very well. The analysis successfully reproduced the seasonal cycle of CO<sub>2</sub> over  
15 Northern Hemisphere mid-latitudes, with low CO<sub>2</sub> concentration in Summer (Figures 7a-  
16 c) and high CO<sub>2</sub> in Winter (Figures 7b-d), consistent with seasonal cycle of CO<sub>2</sub>  
17 absorption and release by terrestrial ecosystems. There are positive CO<sub>2</sub> concentrations  
18 located at high latitudes of North America and far East Asia regions during Winter 2016  
19 (Figure 7f), due to the positive bias in estimated SCF (Figure 6f).

20 The consistency of annual mean estimated SCF for both benchmark experiment  
21 and “truth” is a very important feature for our LETKF\_C assimilation system (Figure 8a).  
22 In EnKF assimilation the ensemble spread is considered as a good representation of  
23 uncertainties associated with both parameters and model state [e.g., Evensen 2007, Liu et  
24 al. 2014]. The surface carbon fluxes are special parameters that vary with time and it is  
25 very hard to quantify their uncertainty during assimilation. When the ensemble spread of  
26 parameters are too small to drive model with a robust response, the estimation fails. The  
27 additive inflation with 30% of nature variability is used to maintain the amplitude of  
28 parameters ensemble spread. Although the ensemble spread of the global total surface  
29 flux, in our experiments, is bigger than its error (Figure 8a), we were still able to estimate  
30 very well the global total surface CO<sub>2</sub> fluxes (ensemble mean), and their seasonal  
31 variability. This is consistent with findings of Liu et al [2014], that parameter estimation

1 can tolerate some inconsistency between parameter ensemble spread and parameter error.

2 The global mean RMSE of SCF decrease from an initial value of  $\sim 0.1$   
3  $kg\ C\ m^{-2}y^{-1}$  to  $\sim 0.04\ kg\ C\ m^{-2}y^{-1}$  in just a few analysis cycles (Figure 8b). It does  
4 not further decrease during following assimilation cycles because the SCF values vary  
5 temporally. The signals added by observations are mainly used to reproduce the temporal  
6 variation of SCF.

7 It is very important for a SCF estimation to reproduce the spatial distribution of  
8 the annual mean of the SCF, since it identifies the carbon sources and sinks in the Earth  
9 System. Though the amplitude of annual mean SCF is much smaller than the seasonal  
10 cycle of SCF, the estimated spatial pattern of annual mean SCF in the benchmark  
11 experiment (Eq. 5) is generally consistent with the “truth” (Figure 9).

$$12\ \Delta F(x) = E_t(F^a(x, t)) - E_t(F^n(x, t))\quad (5)$$

13 In summary, we found that the OSSE experiments using long observation  
14 windows and short assimilation windows resulted in the best estimates of SCF.

15

## 16 **5 Summary and Discussion**

17 We have developed a LETKF-GEOS-Chem carbon data assimilation (LETKF\_C)  
18 system for estimating the surface carbon fluxes (SCF). The “true” GEOS-Chem  
19 atmospheric transport model is driven by the single realization of meteorology fields  
20 from MERRA reanalysis. The proposed data assimilation system captured well the “true”  
21 SCF spatial and temporal variability. The system performed best with a choice of short  
22 assimilation and long observation windows.

23 The LETKF requires a short assimilation window to avoid an ill-posed condition  
24 caused by the nonlinear processes in the forecast model with a long forecast time. The  
25 parameter estimation favors a long training period and many observations. Based on  
26 these features, we developed a new method to accurately estimate the SCF. The new  
27 scheme separates original assimilation time window into observation (OW) and  
28 assimilation (AW) windows, allowing the flexibility to apply an OW that is different than  
29 the AW. Like Running in Place (RIP), the new technique takes advantage of the “no-cost  
30 smoothing” algorithm developed for the LETKF by Kalnay et al. [2007b] that allows to  
31 transport the Kalman Filter solution forward or backward within the observation window.

1 The new method was applied to the LETKF\_C system in the OSSE mode using a  
2 dataset developed based on the OCO-2 observation characteristics. The sensitivity  
3 experiments for this model-assimilation system demonstrated that the new technique, i.e.  
4 using a short AW and long OW, significantly improves the SCF estimation as compared  
5 to regular 4D-LETKF with identical observation and assimilation windows. The best AW  
6 for SCF estimation is 1 day, which is different from the typical AW of 6 hours used in the  
7 meteorological assimilations. An OW in the range of 8-15 days is required to estimate the  
8 surface carbon fluxes for seasonal and longer time scales. The benchmark experiment  
9 with AW of 1 day and the OW of 8 days successfully reproduced the mean seasonal and  
10 annual SCF.

11 Our working hypothesis was that that the optimal OW for the estimation of SCF  
12 could be reduced with more observations. We examined this hypothesis by using  
13 simulated OCO-2 observations and Global View Plus (GV+) observations. Similar to the  
14 OCO-2 pseudo-observations, the GV+ pseudo-observations were also generated based on  
15 the actual location, time and corresponding error scale of the GV+ flask observations.  
16 The results show that the AW/OW lengths of 1day /8 day is also optimal with both the  
17 OCO-2 and GV+ observation characteristics. We estimated the SCF using the OCO-2  
18 and GV+ pseudo-observations with the identical experiment settings as the OCO-2  
19 experiments, except we replace the experiment with very long OW of 30 days with an  
20 experiment with a short OW of 4 days to better evaluate the impact from short OWs.  
21 Thus the current experiments settings are using OW of 2, 4, 8, 15 days.

22 The results from these experiments show that the AW/OW lengths of 1day /8 day  
23 are still optimal for both the OCO-2 and GV+ observation characteristics (Figure 10).  
24 Generally, the time-mean RMSE of estimated SCF with OCO-2 and GV+ (Figure 10) are  
25 smaller than the corresponding estimates for OCO-2 only (Figure 5). The short OW of 2  
26 days performs worse than the moderate OWs of 4 days, 8 days and 15 days. The time-  
27 averaged global mean RMSE is  $0.046 \frac{kgC}{m^2yr}$  for experiments with OW of 2 days (Figure  
28 10a). The time-averaged global mean RMSE is only 0.040, 0.037 and  $0.039 \frac{kgC}{m^2yr}$  for  
29 experiments with OW of 4, 8 and 30 days, respectively (Figure10 b, c and d). We only  
30 see a slight impact of observation coverage on the optimal OW length. The best OW

1 appears to be 8~15 days which produce the smallest RMSE when only OCO-2  
2 observations are assimilated. The smallest RMSE in the experiment is obtained in the  
3 experiment with the best OW of 8 days, when both OCO-2 and GV+ observations are  
4 assimilated into the system.

5 Two different sets of experiments (OCO-2 vs OCO-2 and GV+) suggesting the  
6 same optimal OW of 8 days indicate that the observation coverage and observation type  
7 are not the major factor in deciding the length of optimal OW. We speculate that the  
8 optimal OW is mainly determined by the time-scale of model response to the SCF  
9 uncertainties because LETKF constrains parameters (SCF) based on the mapping  
10 function of parameter-state covariance, hence, only the model response to the parameter  
11 uncertainties provide the signal for parameter estimation.

12 It is worth noting that our approach works best for estimating parameters that vary  
13 slowly over moderate time scales. It may not be optimum for estimating SCF variation  
14 for short time-scales such as sub-daily to daily because the variations shorter than OWs  
15 are filtered out. Furthermore, we used a coarse spatial resolution ( $4^\circ \times 5^\circ$ ) GEOS-Chem  
16 in our study. We postulate that the optimal AW/OW could be different when a higher  
17 spatial resolution version of GEOS-Chem is used with the proposed assimilation system,  
18 because models with different resolutions response to the SCF may be different. This  
19 issue also merits further exploring in the future.

20 Our new developed short AW and long OW technique is different from both the  
21 standard 4D-variational method and the 4D-LETKF. The 4D-Var and the 4D-LETKF  
22 have been shown (Bonavita et al. 2015; Hamrud et al 2015) to have an essentially  
23 equivalent performance, and their hybrid Kalman Gain combination (Penny, 2014) in a  
24 EnKF framework, was comparable to the hybrid ensemble data assimilation system  
25 currently operational at ECMWF, but with lower computational cost. The hybrid  
26 ensemble data assimilation system at ECMWF uses an ensemble of 4D-Var assimilation  
27 at reduced resolution to provide a flow-dependent estimate of background errors for use  
28 in 4D-Var assimilation (Bonavita et al. 2015). The short AW and long OW approach can  
29 be used with other Earth system models for parameter estimation, when the parameters  
30 have slow and smooth variations in time and space, and the observations are too limited  
31 to constrain the parameters well.

1

## 2 **6 Code and data availability**

3 This study focused on developing a new methodology for estimating carbon flux  
4 based on a carbon cycle model/data assimilation system. It does not generate any new  
5 dataset. The related code for GEOS-Chem and LETKF can be accessed from  
6 [http://acmg.seas.harvard.edu/geos/doc/man/chapter\\_2.html#DownCode](http://acmg.seas.harvard.edu/geos/doc/man/chapter_2.html#DownCode) and  
7 <https://github.com/takemasa-miyoshi/letkf>, respectively.

8

## 9 **Acknowledgment**

10 This research is sponsored by NOAA OAR (NA18OAR4310266 and NA10OAR4310248)  
11 and NASA (80NSSC18K0908 and NNX15AG95G). It is also partial supported by  
12 Laboratory Directed Research and Development funding by The Pacific Northwest  
13 National Laboratory (PNNL), managed by the Battelle Memorial Institute for the US  
14 Department of Energy.

15

16

## 17 **References:**

18 Anderson, J.L.: An ensemble adjustment Kalman filter for data assimilation. *Mon. Wea.*  
19 *Rev.*, 129, 2884–2903, 2001.

20 Anderson J.L.: A local least squares framework for ensemble filtering. *Mon. Wea. Rev.*,  
21 131, 634–642, 2003.

22 Anderson, J. L., and Anderson, S. L.: A Monte Carlo implementation of the nonlinear  
23 filtering problem to produce ensemble assimilations and forecasts, *Mon. Weather Rev.*,  
24 127, 2741–2758, doi:10.1175/15200493(1999)127<2741:AMCIOT>2.0.CO;2, 1999.

25 Asefi-Najafabady, S., Rayner, P. J., Gurney, K. R., McRobert, A., Song, Y., Coltin, K.,  
26 Huang, J., Elvidge, C., and Baugh, K.: A multiyear, global gridded fossil fuel CO<sub>2</sub>  
27 emission data product: Evaluation and analysis of results, *J. Geophys. Res. Atmos.*, 119,  
28 10,213–10,231, doi:10.1002/2013JD021296, 2014.

29 Banks, H.T.: Control and estimation in distributed parameter systems. In: H.T. Banks,  
30 Editor, *Frontiers in Applied Mathematics* vol. 11, SIAM, Philadelphia, pp 227, 1992a.

1 Banks, H.T.: Computational issues in parameter estimation and feedback control  
2 problems for partial differential equation systems. *Physica D* 60, 226-238, 1992b.

3 Baker, D. F., Doney, S. C., and Schimel, D. S.: Variational data assimilation for  
4 atmospheric CO<sub>2</sub>, *Tellus, Ser. B*, 58, 359–365, doi:10.1111/j.1600-0889.2006.00218.x,  
5 2006.

6 Baker, D. F., Bösch, H., Doney, S. C., O’Brien, D., and Schimel D. S.: Carbon  
7 source/sink information provided by column CO<sub>2</sub> measurements from the Orbiting  
8 Carbon Observatory, *Atmos. Chem. Phys.*, 10, 4145–4165, doi:10.5194/acp-10-4145-  
9 2010, 2010.

10 Basu, S., Baker, D. F., Chevallier, F., Patra, P. K., Liu, J., and Miller, J. B.: The impact of  
11 transport model differences on CO<sub>2</sub> surface flux estimates from OCO-2 retrievals of  
12 column average CO<sub>2</sub>, *Atmos. Chem. Phys.*, 18, 7189-7215, [https://doi.org/10.5194/acp-](https://doi.org/10.5194/acp-18-7189-2018)  
13 18-7189-2018, 2018.

14 Bey, I., Jacob, D. J., Yantosca, R. M., Logan, J. A., Field, B., Fiore, A. M., Li, Q., Liu,  
15 H., Mickley, L. J., and Schultz M.: Global modeling of tropospheric chemistry with  
16 assimilated meteorology: Model description and evaluation, *J. Geophys. Res.*, 106,  
17 23,073-23,096, 2001.

18 Nassar, R., Napier-Linton, L., Gurney, K.R., Andres, R.J., Oda, T., Vogel, F.R., and  
19 Deng, F.: Improving the temporal and spatial distribution of CO<sub>2</sub> emissions from global  
20 fossil fuel emission data sets, *J. Geophys. Res. Atmos.*, 118, 917-933,  
21 doi:10.1029/2012JD018196, 2013.

22 Bishop, C. H., Etherton, B. J., and Majumdar, S. J.: Adaptive sampling with the ensemble  
23 transformation kalman filter. Part i: theoretical aspects. *Mon. Wea. Rev.*, 129, 420–436,  
24 2001.

25 Bosilovich, M. G., Akella, S., Coy, L. et al.: MERRA-2: Initial evaluation of the climate.  
26 Series on Global Modeling and Data Assimilation, NASA/TM, 104606, 2015.

27 Bonavita M. G., Hamrud, M., and Isaksen, L.: EnKF and hybrid gain ensemble data  
28 assimilation. Part II: EnKF and hybrid gain results. *Mon. Wea. Rev.*, 143, 4865–4882,  
29 doi:10.1175/MWR-D-15-0071.1, 2015.

30 Burgers, G., Van Leeuwen, P., Evensen, G.: Analysis scheme in the ensemble Kalman  
31 filter. *Mon. Wea. Rev.*, 126, 1719–1724, 1998.

1 Chevallier, F., Engelen, R. J., Carouge, C., Conway, T. J., Peylin, P., Pickett-Heaps, C.,  
2 Ramonet, M., Rayner, P. J., and Xueref-Remy I.: AIRS-based versus flask-based  
3 estimation of carbon surface fluxes, *J. Geophys. Res.*, 114, D20303,  
4 doi:10.1029/2009JD012311, 2009.

5 Cooperative Global Atmospheric Data Integration Project: Multi-laboratory compilation  
6 of atmospheric carbon dioxide data for the period 1957-2015;  
7 obspack\_co2\_1\_GLOBALVIEWplus\_v2.1\_2016\_09\_02; NOAA Earth System Research  
8 Laboratory, Global Monitoring Division. <http://dx.doi.org/10.15138/G3059Z>, 2016.

9 Crisp, D., Randerson, J. T., Wennberg, P. O., Yung, Y. L., and Kuang, Z.: The Orbiting  
10 Carbon Observatory (OCO) mission, *Adv. Space Res.*, 34, 700–709,  
11 doi:10.1016/j.asr.2003.08.062, 2004.

12 Evensen G.: Sequential data assimilation with a non-linear quasi-geostrophic model using  
13 Monte Carlo methods to forecast error statistics. *J. Geophys. Res.*, 99(C5), 10143–10162,  
14 1994.

15 Enting, I. G.: *Inverse Problems in Atmospheric Constituent Transport*, Cambridge Univ.  
16 Press, New York, doi:10.1017/CBO9780511535741, 2002.

17 Feng, L., Palmer, P. I., Bösch, H., and Dance S.: Estimating surface CO<sub>2</sub> fluxes from  
18 space-borne CO<sub>2</sub> dry air mole fraction observations using an ensemble Kalman filter,  
19 *Atmos. Chem. Phys.*, 9, 2619–2633, doi:10.5194/acp-9-2619-2009, 2009.

20 Hamrud M., Bonavita M., and Isaksen, L.: EnKF and Hybrid Gain Ensemble Data  
21 Assimilation. Part I: EnKF Implementation. *Mon Wea Rev.*, DOI: 10.1175/MWR-D-14-  
22 00333.1, 2015.

23 Harlim, J. and Hunt, B. R.: Four-dimensional local ensemble transform Kalman filter:  
24 numerical experiments with a global circulation model. *Tellus A*, 59: 731–748.  
25 doi:10.1111/j.1600-0870.2007.00255.x, 2007.

26 Houtekamer, P. L., Mitchell, H. L.: Data assimilation using an ensemble Kalman filter  
27 technique. *Mon. Wea. Rev.*, 126, 796–811., 1998.

28 Hunt, B. R., Kostelich, E., and Szunyogh, I.: Efficient data assimilation for  
29 spatiotemporal chaos: A local ensemble transform Kalman filter, *Physica D*, 230, 112–  
30 126, doi:10.1016/j.physd.2006.11.008, 2007.

31 Liu, J., K. W. Bowman, and M. Lee: Comparison between the Local Ensemble



1 Transform Kalman Filter (LETKF) and 4D-Var in atmospheric CO<sub>2</sub> flux inversion with  
2 the Goddard Earth Observing System-Chem model and the observation impact  
3 diagnostics from the LETKF, *J. Geophys. Res. Atmos.*, 121,13,066–13,087,  
4 doi:10.1002/2016JD025100, 2016.

5 Liu Y., Liu, Z., Zhang, S., Jacob, R., Lu, F., Rong, X., Wu, S.: Ensemble-Based  
6 Parameter Estimation in a Coupled General Circulation Model. *Journal of climate*, 27,  
7 7151–7162, 2014.

8 Le Quéré, C., Moriarty, R., Andrew, R. M. et al.: Global carbon budget 2014, *Earth Syst.*  
9 *Sci. Data*, 7, 47-85, doi:10.5194/essd-7-47-2015, 2015.

10 Le Quéré C., Andrew, R. M., Canadell, J. G. et al.: Global Carbon Budget 2016, *Earth*  
11 *Syst. Sci. Data*, 8, 605-649, doi:10.5194/essd-8-605-2016, 2016.

12 Lokupitiya, R. S., Zupanski, D., Denning, A. S., Kawa, S. R., Gurney, K. R., and  
13 Zupanski M.: Estimation of global CO<sub>2</sub> fluxes at regional scale using the maximum  
14 likelihood ensemble filter, *J. Geophys. Res.*, 113, D20110, doi:10.1029/2007JD009679,  
15 2008.

16 Kalnay E., Li, H., Miyoshi, T., Yang, S.-C., and Ballabrera-Poy, J.: 4-D-Var or ensemble  
17 Kalman filter?. *Tellus, Ser. A*, 59, 758–773, doi:10.1111/j.1600-0870.2007.00261.x,  
18 2007a.

19 Kalnay E., Li, H., Miyoshi, T., Yang, S.-C., and Ballabrera-Poy, J.: Response to the  
20 discussion on “4-D-Var or EnKF?” by Nils Gustafsson. *Tellus, Ser. A*, 59, 778-780, doi:  
21 10.1111/j.1600-0870.2007.00263.x, 2007b.

22 Kalnay, E. and Yang, S.-C.: Accelerating the spin-up of Ensemble Kalman Filtering.  
23 *Q.J.R. Meteorol. Soc.*, 136: 1644–1651. doi:10.1002/qj.652, 2010.

24 Kang, J.-S., Kalnay, E., Liu, J., Fung, I., Miyoshi, T., and Ide, K.: “Variable localization”  
25 in an ensemble Kalman filter: Application to the carbon cycle data assimilation, *J.*  
26 *Geophys. Res.*, 116, D09110, doi:10.1029/2010JD014673., 2011.

27 Kang J.-S., Kalnay, E., Miyoshi, T., Liu, J., Fung, I.: Estimation of surface carbon fluxes  
28 with an advanced data assimilation methodology: SURFACE CO<sub>2</sub> FLUX  
29 ESTIMATION. *Journal of geophysical research*, 117., doi:10.1029/2012JD018259, 2012.

30 Mitchell, H. L., and Houtekamer, P. L.: An adaptive ensemble Kalman filter. *Mon. Wea.*  
31 *Rev.*, 128, 416–433, 2000.

1 Michalak, A. M.: Adapting a fixed-lag Kalman smoother to a geostatistical atmospheric  
2 inversion framework, *Atmos. Chem. Phys.*, 8, 6789–6799, 2008.

3 Miyoshi, T.: The Gaussian approach to adaptive covariance inflation and its  
4 implementation with the local ensemble transform Kalman filter. *Mon. Wea.*  
5 *Rev.*, 139, 1519–1535, doi:10.1175/2010MWR3570.1, 2011.

6 O'Dell, C. W., Connor, B., Bösch, H., O'Brien, D., Frankenberg, C., Castano, R., Christi,  
7 M., Eldering, D., Fisher, B., Gunson, M., McDuffie, J., Miller, C. E., Natraj, V., Oyafuso,  
8 F., Polonsky, I., Smyth, M., Taylor, T., Toon, G. C., Wennberg, P. O., and Wunch, D.:  
9 The ACOS CO<sub>2</sub> retrieval algorithm – Part 1: Description and validation against synthetic  
10 observations, *Atmos. Meas. Tech.*, 5, 99–121, doi:10.5194/amt-5-99-2012, 2012

11 Penny, S.G.: The Hybrid Local Ensemble Transform Kalman Filter. *Mon. Wea. Rev.*,  
12 142, 2139–2149, 2014.

13 Peters, W., Miller, J. B., Whitaker, J., Denning, A. S., Hirsch, A., Krol, M. C., Zupanski,  
14 D., Bruhwiler, L., and Tans, P. P.: An ensemble data assimilation system to estimate CO<sub>2</sub>  
15 surface fluxes from atmospheric trace gas observations, *J. Geophys. Res.*, 110, D24304,  
16 doi:10.1029/2005JD006157, 2005.

17 Peters, W., Jacobson, A.R., Sweeney, C. et al.: An atmospheric perspective on North  
18 American carbon dioxide exchange: Carbon tracker, *Proc. Natl. Acad. Sci. U. S. A.*, 104,  
19 18,925–18,930, doi:10.1073/pnas.0708986104, 2007.

20 Tippett, M., Anderson, J. L., Bishop, C. H., Hamill, T. M., Whitaker, J. S.: Ensemble  
21 square root filters. *Mon. Wea. Rev.*, 131, 1485–1490, 2003.

22 Wang, S., Xue, M., Schenkman, A. D., and Min, J.: An iterative ensemble square root  
23 filter and tests with simulated radar data for storm scale data assimilation. *Quart. J. Roy.*  
24 *Meteor. Soc.*, 139, 1888–1903, 2013.

25 Whitaker, J. S., and Hamill, T. M.: Ensemble data assimilation without perturbed  
26 observations. *Mon. Wea. Rev.*, 130, 1913–1924., 2002.

27 Whitaker J. S., Wei, X., Song, Y., and Toth, Z.: Ensemble data assimilation with the  
28 NCEP global forecast system. *Mon. Wea. Rev.*, 136, 463–482, 2008.

29 Yang, S., Kalnay, E., and Miyoshi T.: Accelerating the EnKF Spinup for Typhoon  
30 Assimilation and Prediction. *Wea. Forecasting*, 27, 878–897,  
31 <https://doi.org/10.1175/WAF-D-11-00153.1>, 2012.

32 Yokota, T., Oguma, H., Morino, I., and Inoue, G.: A nadir looking SWIR FTS to monitor

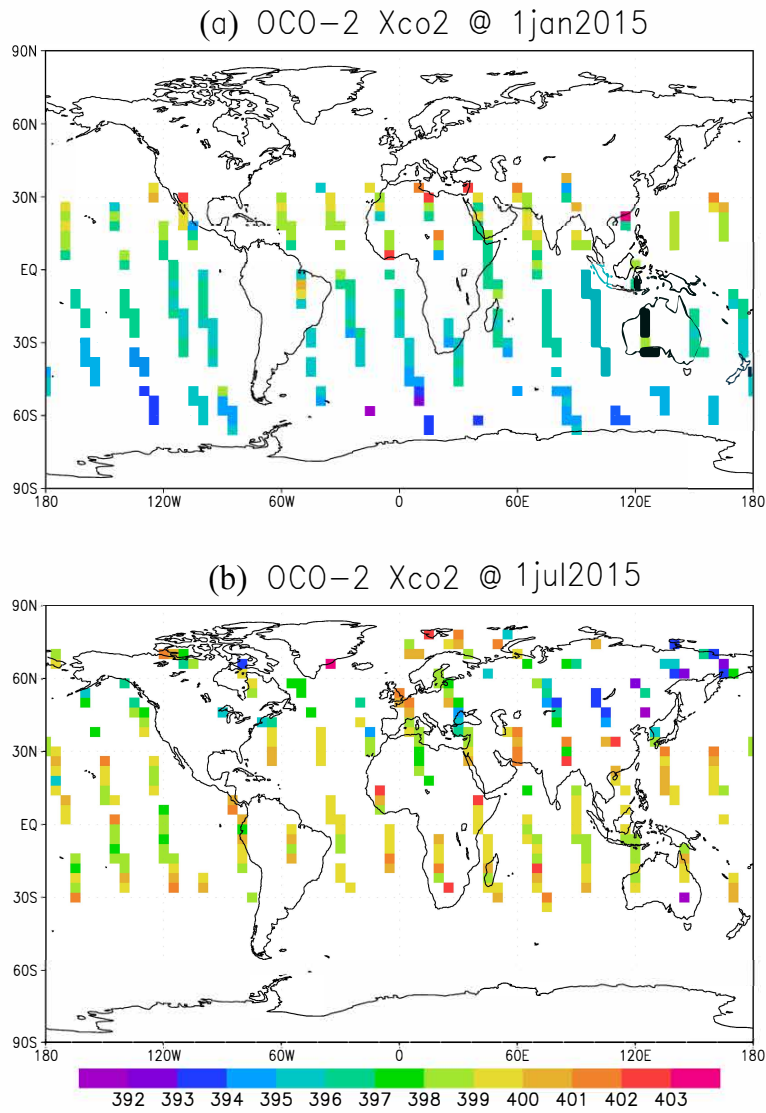
1 CO<sub>2</sub> column density for Japanese GOSAT project, in Proceedings of the Twenty-fourth  
2 International Symposium on Space Technology and Science (Selected Papers), pp. 887–  
3 889, Jpn. Soc. for Aeronaut. and Space Sci., Tokyo, 2004.

4 Zeng, N., Mariotti, A., and Wetzel, P.: Terrestrial mechanisms of interannual CO<sub>2</sub>  
5 variability, *Global Biogeochemical Cycles*, 19, GB1016, doi:10.1029/2004GB002273,  
6 2005

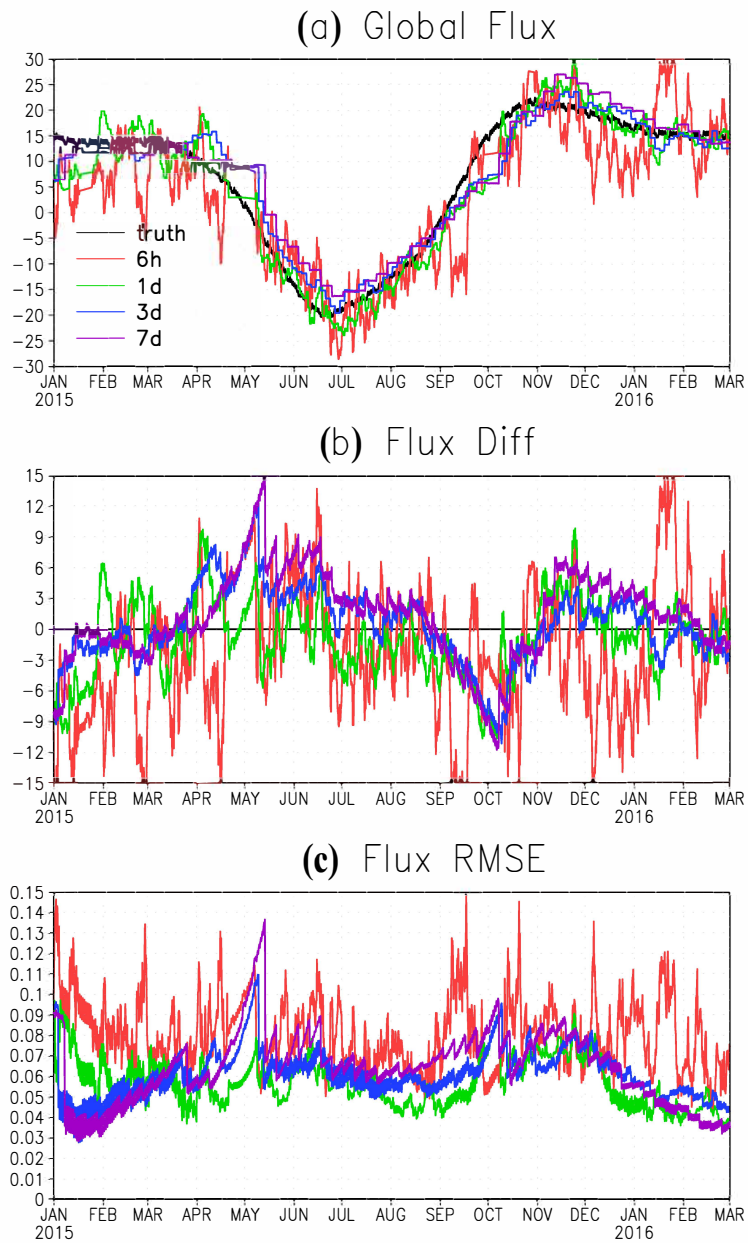
7 Zeng, N., Qian, H., Munoz, E., and Iacono, R.: How strong is carbon cycle-climate  
8 feedback under global warming? *Geophys. Res. Lett.*, 31 L20203,  
9 doi:10.1029/2004GL020904, 2004.

10 Zhang, F., Snyder, C., and Sun, J.: Impacts of initial estimate and observation availability  
11 on convective-scale data assimilation with an ensemble Kalman filter. *Mon. Wea. Rev.*,  
12 132, 1238–1253, 2004.

13 Zupanski, D., Denning, A. S., Uliasz, M., Zupanski, M., Schuh, A. E., Rayner, P. J.,  
14 Peters, W., and Corbin, K. D.: Carbon flux bias estimation employing Maximum  
15 Likelihood Ensemble Filter (MLEF), *J. Geophys. Res.*, 112, D17107,  
16 doi:10.1029/2006JD008371. 2007.

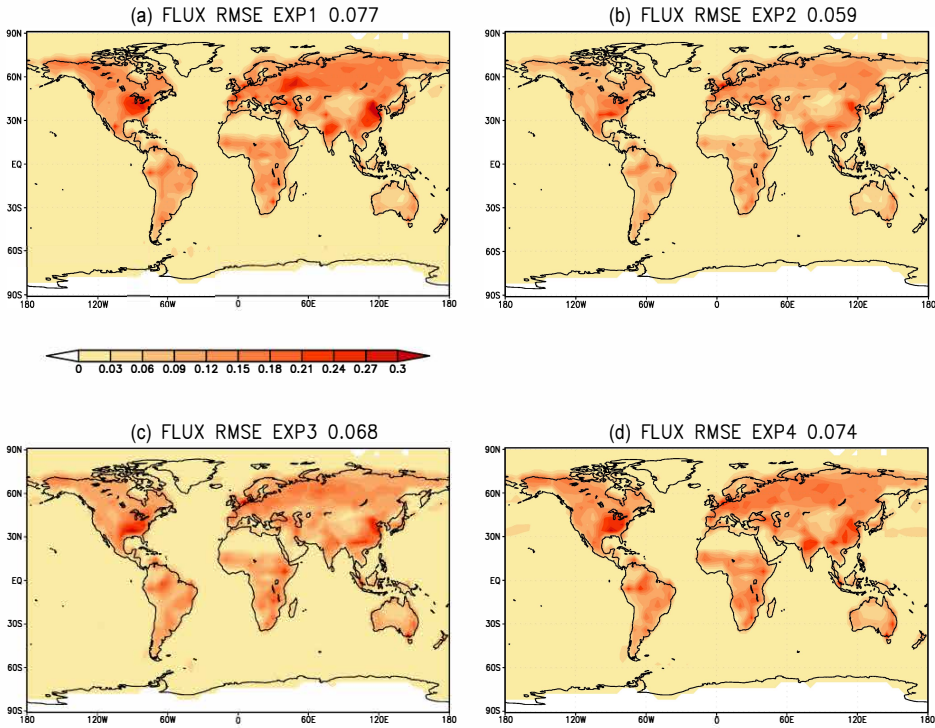


1  
 2 Figure 1. The 10-seconds average of good quality OCO-2 Xco2 observations (Warning  
 3 Level  $\leq 15$ ), obtained from David Baker for (a) 1 January 2015 and (b) 1 July 2015.  
 4  
 5



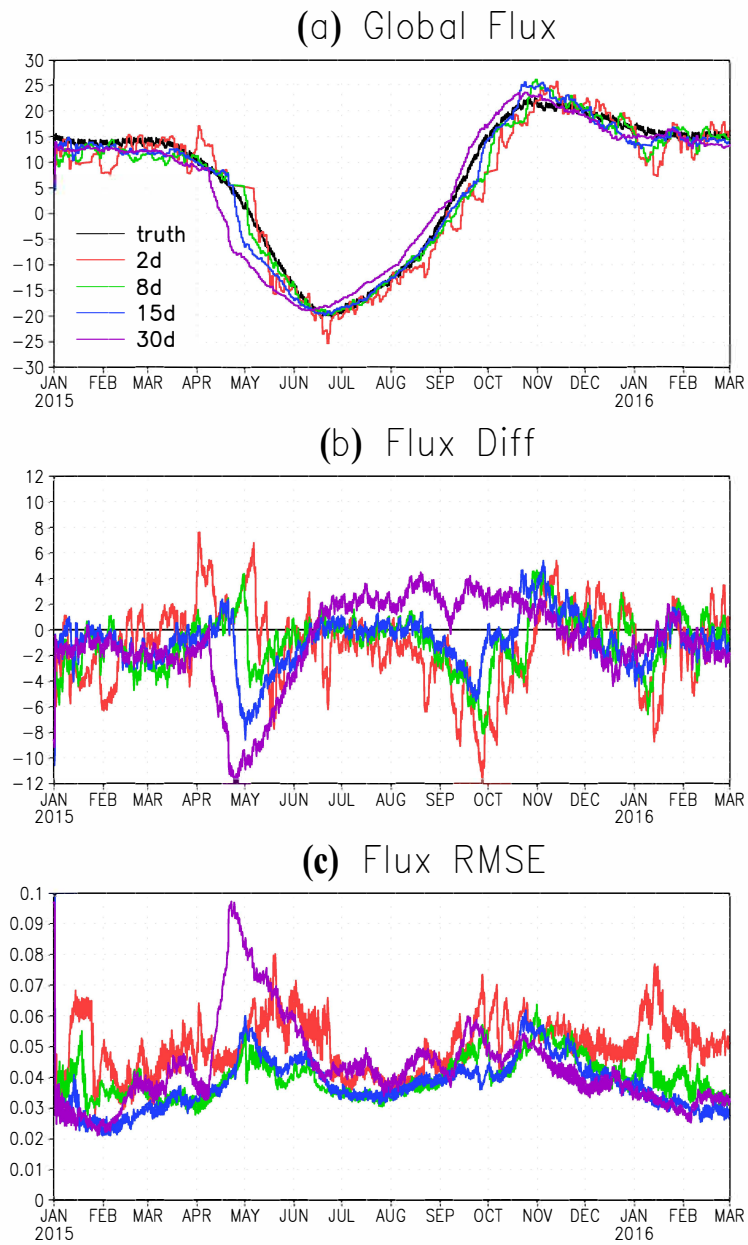
1  
 2 Figure 2. (a) the global total SCF from nature run (“truth”, black line) and from the  
 3 estimations of the first set of experiments with different AW. (b) the difference of global  
 4 total SCF between the estimations from the experiments with different AW and the  
 5 nature run (“truth”). (c) the global average RMSE of the estimated SCFs from the  
 6 experiments with different AW.  
 7

Fnet RMSE of AW 6h/1d/3d/7d 06z01mar2015–01mar2016



1  
2 Figure 3. The spatial pattern of the annual mean RMSE of estimated SCF from the  
3 experiments with different AW (EXP1-4) for the average period from 1 March 2015 to  
4 the end of February 2016. (January and February 2015 are treated as spinup period for  
5 our experiments).  
6

1



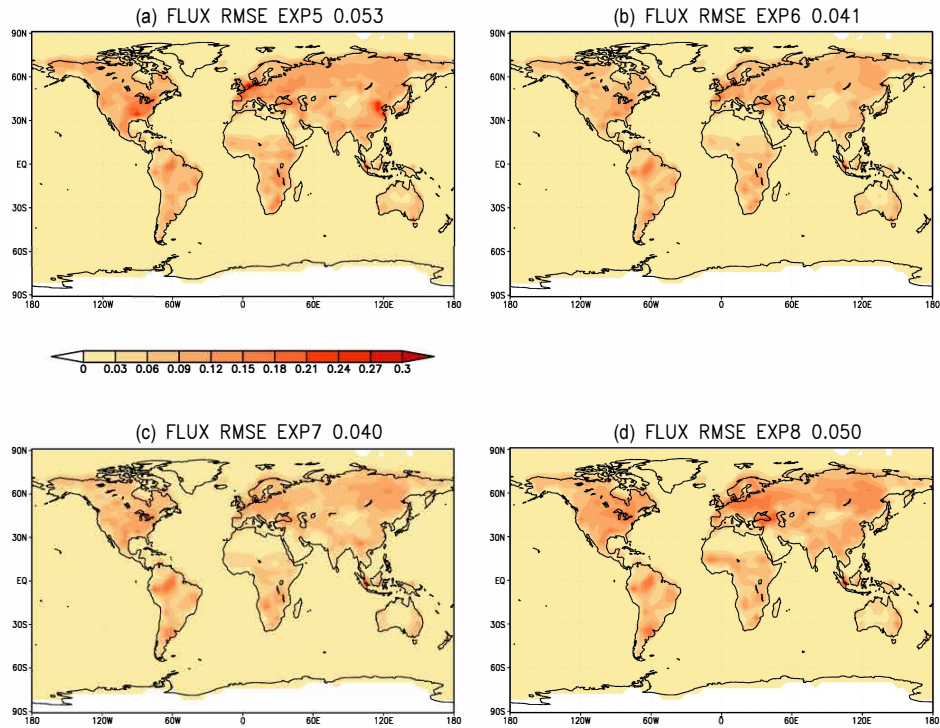
2

3 Figure 4. Same as Figure 2, except for the second set of experiments with different OW,  
4 but same AW of 1 day.

5

1

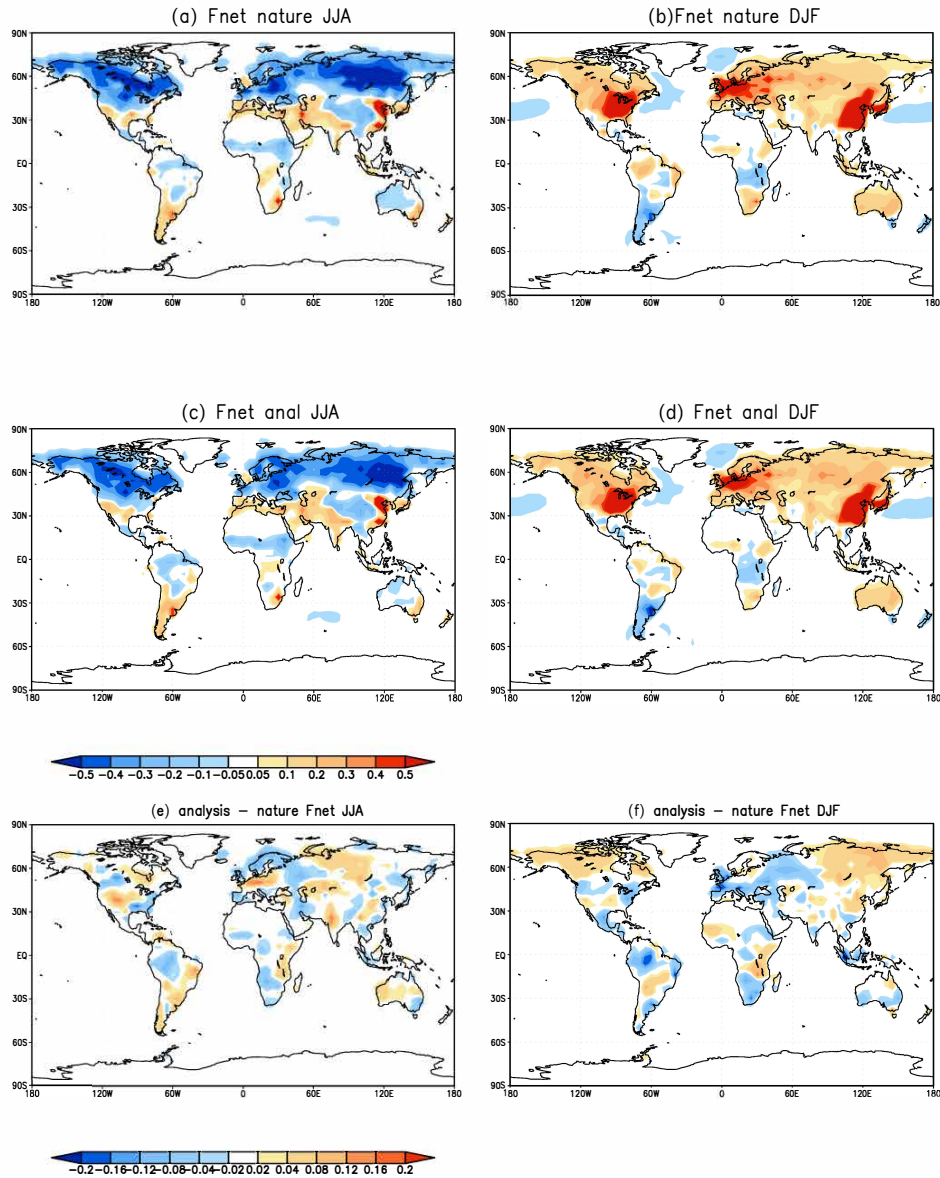
**Fnet RMSE of OW 2d/8d/15d/30d 06z01mar2015–01mar2016**



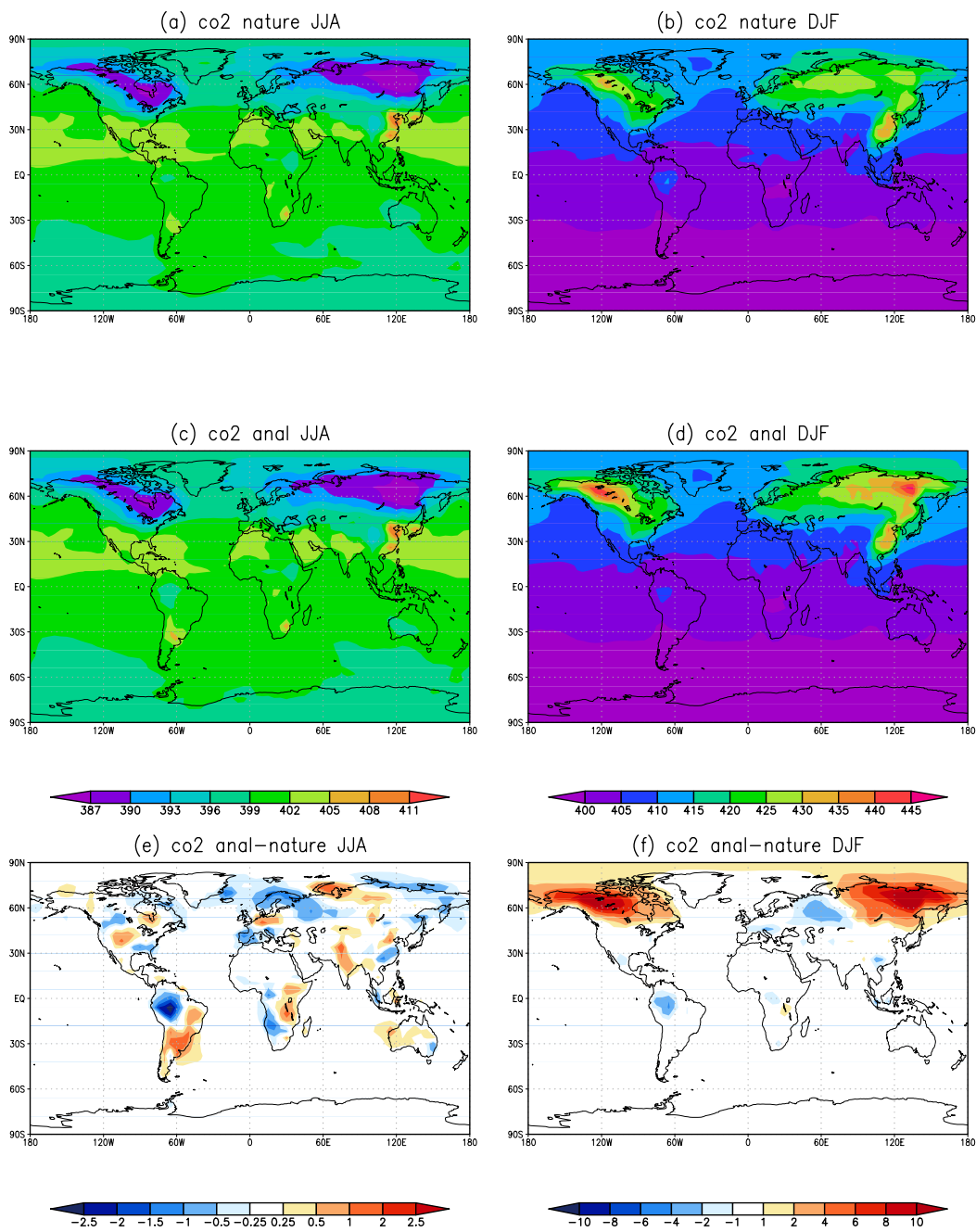
2  
3  
4  
5  
6  
7

Figure 5. Same as Figure 3, except for the second set of experiments with different OW, but similar AW of 1 day.

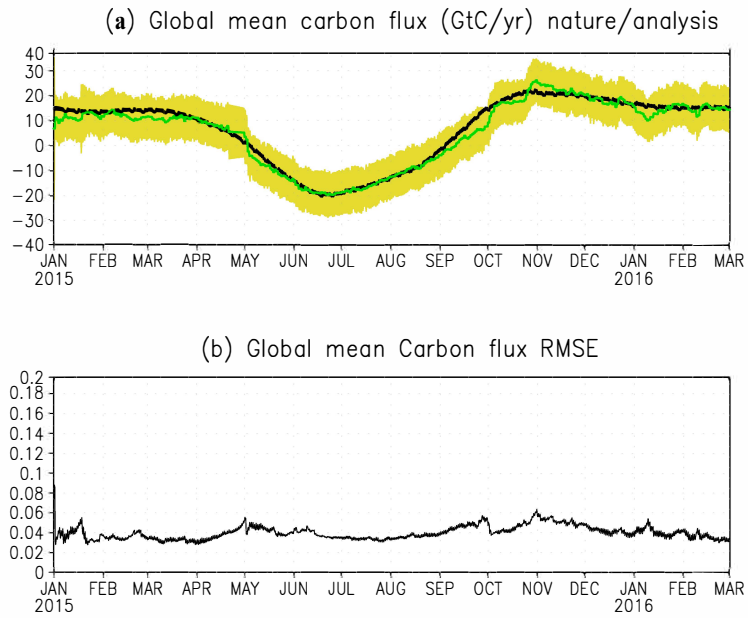




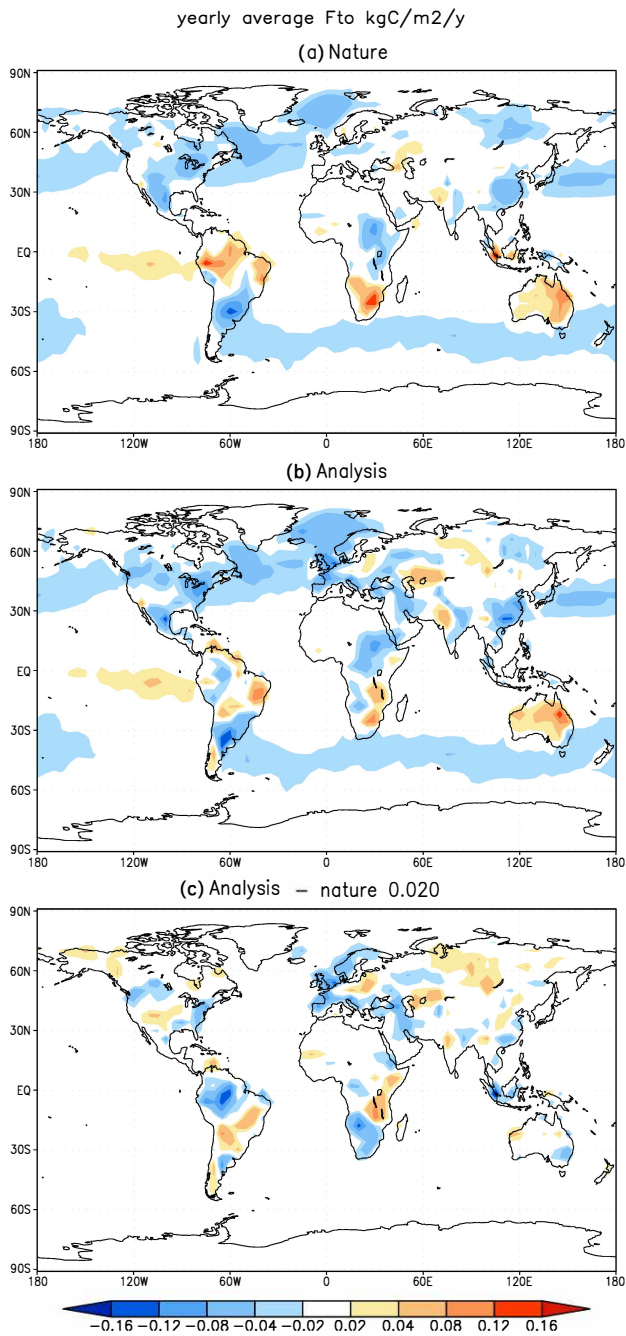
1  
2 Figure 6. The SCF of “nature” run and estimation from benchmark experiment for  
3 Northern Hemisphere Summer (a, c and e), and Winter (b, d, and f). The a and b are the  
4 “truth” from the “nature” run; the c and d are the estimates from benchmark experiment;  
5 and the e and f are the difference between estimation and “truth”.  
6



1  
 2 Figure 7. Same as Figure 6, except for surface concentrations of CO<sub>2</sub>. Where (a) and (c)  
 3 share the upper left colorbar; (b) and (d) use the upper right colorbar.  
 4



1  
 2 Figure 8. (a) The global total SCF of “truth” and estimation from the benchmark  
 3 experiment: the black line is the truth, green line is the ensemble mean of the estimation,  
 4 and yellow shading is the ensemble spread. (b) the global mean RMSE of the estimated  
 5 SCF from the benchmark experiment.  
 6

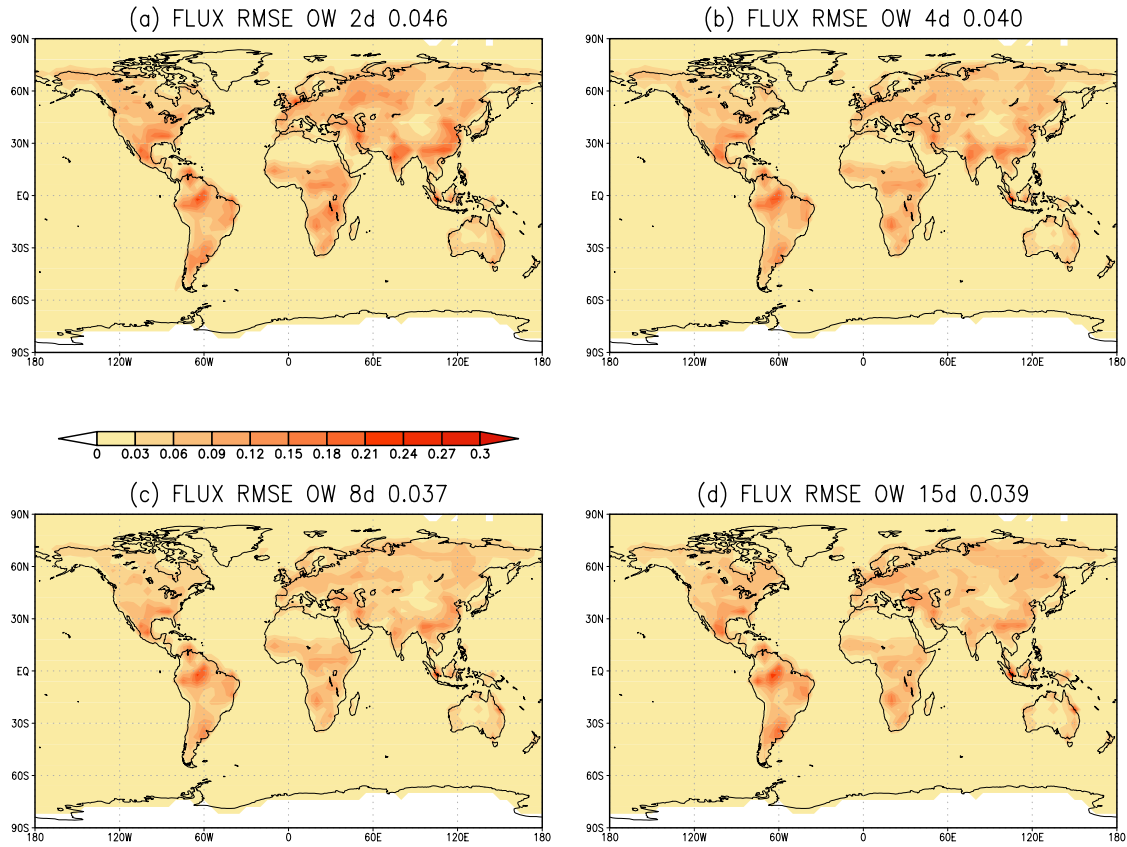


1  
 2 Figure 9. (a) the annual mean of SCF (with the FFE removed) for “nature” run; (b) the  
 3 annual mean of estimated SCF (with the FFE removed) from benchmark experiment ;  
 4 and (c) their differences.

5  
 6  
 7

1  
2  
3

Fnet RMSE of OW 2d/4d/8d/15d using OCO2 and GV+



4  
5 Figure 10. Same as Figure 5, except for assimilating both OCO-2 and GV+ Pseudo-  
6 Observations. The panel (a), (b), (c) and (d) show the results with OW of 2 days, 4 days,  
7 8 days and 15 days respective.